



# Open Research Online

---

The Open University's repository of research publications and other research outputs

## Direct e-beam lithography of PDMS

### Conference or Workshop Item

#### How to cite:

Bowen, J.; Cheneler, D. and Robinson, A. P. G. (2011). Direct e-beam lithography of PDMS. In: 37th International Conference on Micro and Nano Engineering, 19-22 Sep 2011, Berlin, Germany.

For guidance on citations see [FAQs](#).

© 2011 The Authors

Version: Version of Record

Link(s) to article on publisher's website:

[https://www.academia.edu/9823134/Direct\\_e-beam\\_lithography\\_of\\_PDMS](https://www.academia.edu/9823134/Direct_e-beam_lithography_of_PDMS)

---

Copyright and Moral Rights for the articles on this site are retained by the individual authors and/or other copyright owners. For more information on Open Research Online's data [policy](#) on reuse of materials please consult the policies page.

---

[oro.open.ac.uk](http://oro.open.ac.uk)



# Direct E-beam Lithography of PDMS

J. Bowen<sup>a</sup>, D. Cheneler<sup>b</sup>, A. P. G. Robinson<sup>a</sup>

<sup>a</sup> School of Chemical Engineering, University of Birmingham, Birmingham, B15 2TT, UK

<sup>b</sup> School of Mechanical Engineering, University of Birmingham, Birmingham, B15 2TT, UK

## Introduction

Poly-(dimethyl siloxane) (PDMS) is a versatile material frequently used in the fabrication of micro and nano scale devices. It has a unique combination of properties including excellent thermal and chemical stability and non-toxicity making it an attractive material for use in many fields of science, especially in biomedical research [1]. Its sensitivity to electron radiation [2] has lead to its use as a resist for subsequent substrate patterning [3] albeit generally in a modified form [4-6]. Here we analyze the effects of exposing liquid PDMS to electron radiation over a large range of doses on the resulting elastic modulus and topography. The data shows that PDMS processed using e-beam lithographic techniques is a viable structural material capable of being utilized in the next generation of microfluidic and other micro devices.

## Fabrication by E-Beam Lithography

PDMS with a zero shear viscosity of 1 Pa.s was decanted onto a clean Si wafers (IDB Technologies, UK; 2 nm native SiO<sub>2</sub> layer) and spun at a frequency of 33.3 Hz for 100 minutes, using a spin processor (WS-400E-6NPP-Lite, Laurell Technologies, USA). The resultant PDMS film thickness were in the range 1.1  $\mu\text{m} \pm 50$  nm and measured using an ellipsometer (UVISSEL, Horiba Scientific) operating over the wavelength range 250 – 800 nm. Exposure was carried out using an FEI XL30 SFEG field emission scanning electron microscope (SEM) equipped with a pattern generator for lithography (Raith Elphy Plus). Arrays of 25 squares of 50 x 50  $\mu\text{m}$  was exposed on the sample at a beam energy of 30 keV and beam current 1.02 nA, using the Raith pattern generator. After exposure the sample was dipped in toluene for 10 seconds to remove the unexposed areas of the PDMS from the substrate. Visualisation of topography (see Figs. 1 and 2) was performed using a MicroXAM2 interferometer (Omniscan, UK).

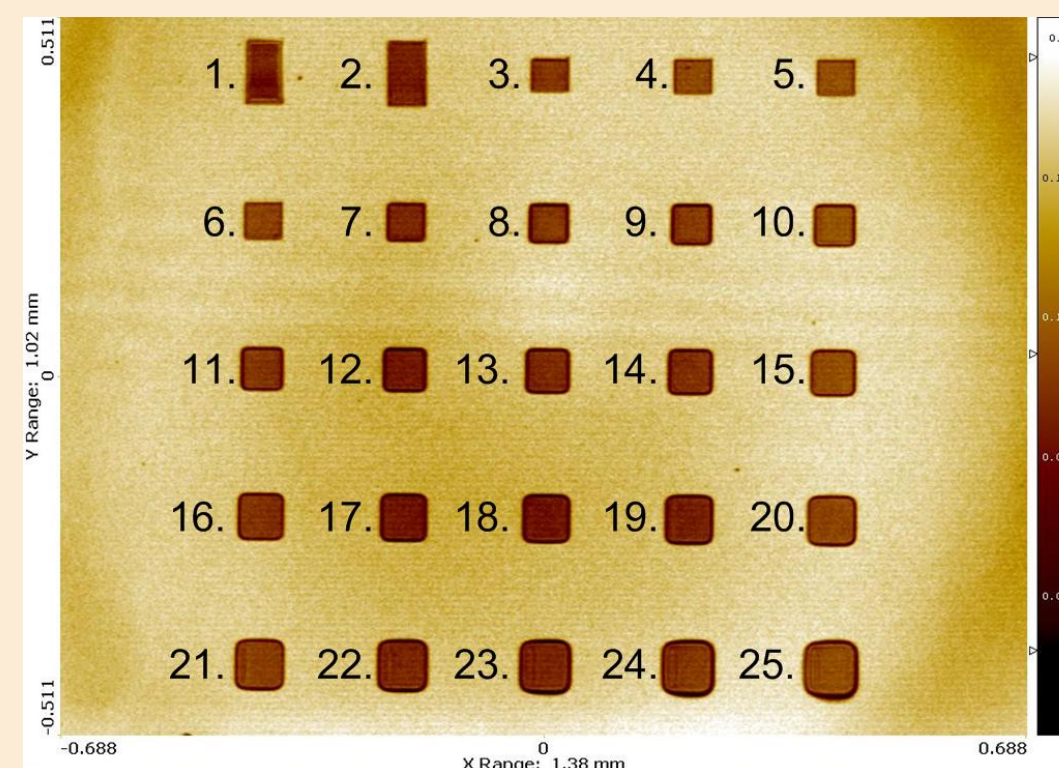


Fig. 1: Topography of PDMS irradiated with dose range 10-10,000  $\mu\text{C}/\text{cm}^2$

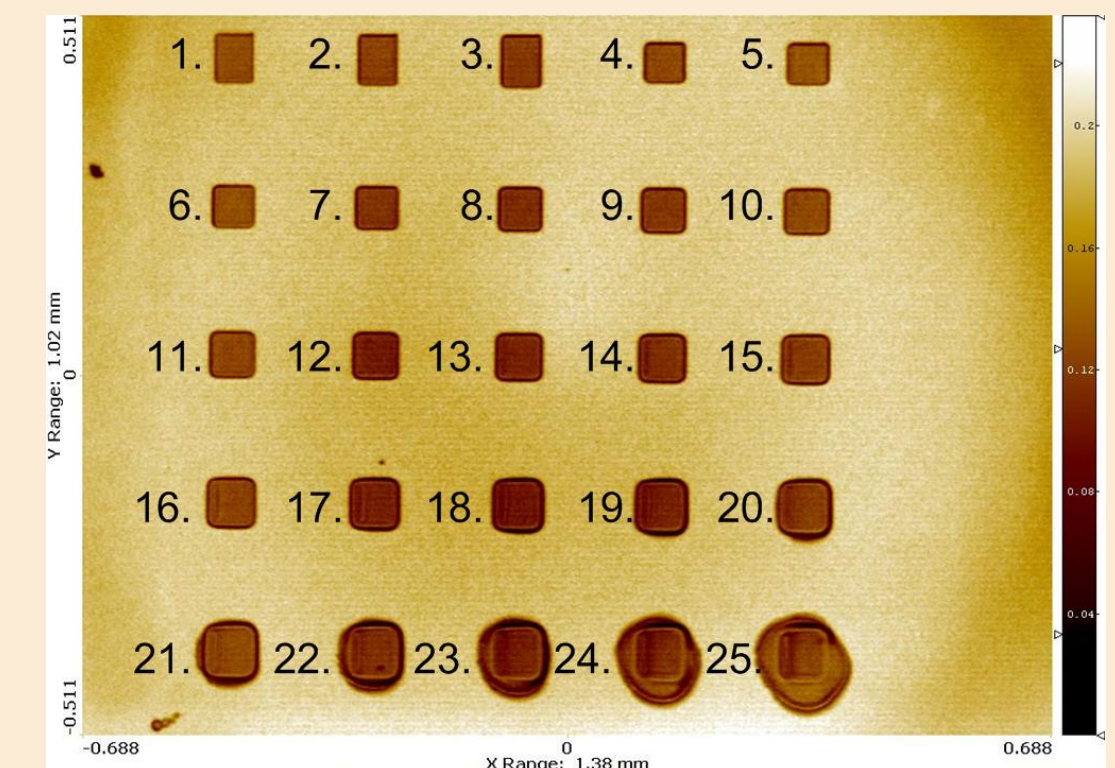


Fig. 2: Topography of PDMS irradiated with dose range 50-50,000  $\mu\text{C}/\text{cm}^2$

## Experimental Analysis of Topography and Elastic Modulus

Acquisition of topographical and mechanical data were performed simultaneously using a NanoWizard II AFM (JPK, UK) operating in force scan mapping mode, at a temperature of 18 °C and a relative humidity in the range 25-35 %. This involved the use of a scanner with a maximum lateral range of 100 x 100  $\mu\text{m}$  and a maximum vertical range of 90  $\mu\text{m}$  in conjunction with a CellHesion module (JPK, UK). Data acquisition was performed using rectangular 130  $\mu\text{m}$  length Si cantilevers (type NSC36/no Al, Mikro Masch, Estonia) having pyramidal tips with 10 nm nominal radii of curvature. Cantilever spring constants were on the order 0.2 N/m and were calibrated according to the method reported by Bowen *et al.* [7]. Data were acquired at 400 surface locations within the 100 x 100  $\mu\text{m}$  scan area by driving the fixed end of the cantilever at a velocity of 20  $\mu\text{m}/\text{s}$  towards the sample surface, whilst monitoring the deflection of the free end of the cantilever using a laser beam. Upon making contact with a surface feature, the height of the contact point was recorded, which was converted into a map of surface topography. A Hertzian model was fitted to data from four separated positions to assess the mechanical response of each exposed region. A maximum compressive load of 5 nN was applied to the surface during data acquisition, which corresponded to a small indentation strain.

The data in Fig. 3 shows how the Young's modulus generally increases with increasing dose. At doses below c.a. 150  $\mu\text{C}/\text{cm}^2$  the PDMS appears to be still mostly liquid-like with the apparent increase in elastic modulus corresponding to a change in the viscoelastic properties of the material. The noise at very low doses suggests that there is local agglomeration of partially cross-linked polymer chains through which the indentation is affected by the proximity of the substrate. The discontinuity at c.a. 150  $\mu\text{C}/\text{cm}^2$  implies a critical cross-linking density at which solidification occurs. Topology data measured with the AFM, as exemplified in Fig. 4, was used to measure the thickness of the PDMS remaining after development. Fig. 5 shows that at doses above the critical value of c.a. 150  $\mu\text{C}/\text{cm}^2$ , the resultant thickness plateaus to a value close to that of the liquid film. The noise at doses above c.a. 3000  $\mu\text{C}/\text{cm}^2$  in Fig. 3 is due to swelling effects due to excessive backscattering corresponding to the increase in thickness in Fig. 5 and reduction in resolution as seen in Figs. 1 and 2. This suggests that between the limits of 150  $\mu\text{C}/\text{cm}^2$  and 3000  $\mu\text{C}/\text{cm}^2$ , the PDMS is solid with consistent thickness and resolution and that the Young's modulus is adjustable by three orders of magnitude from 1 MPa to 1 GPa.

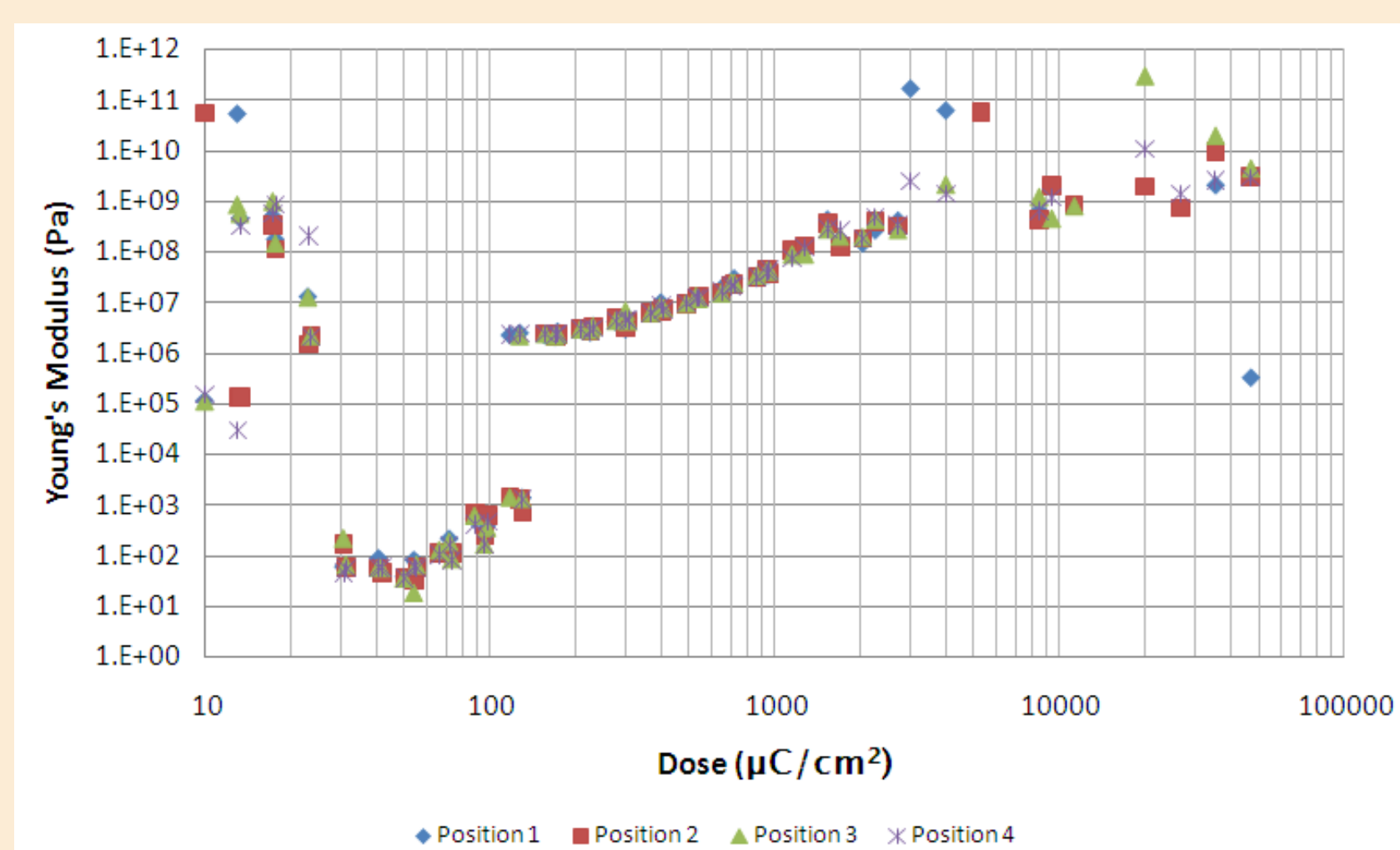


Fig. 3: Effect of dose on Young's modulus

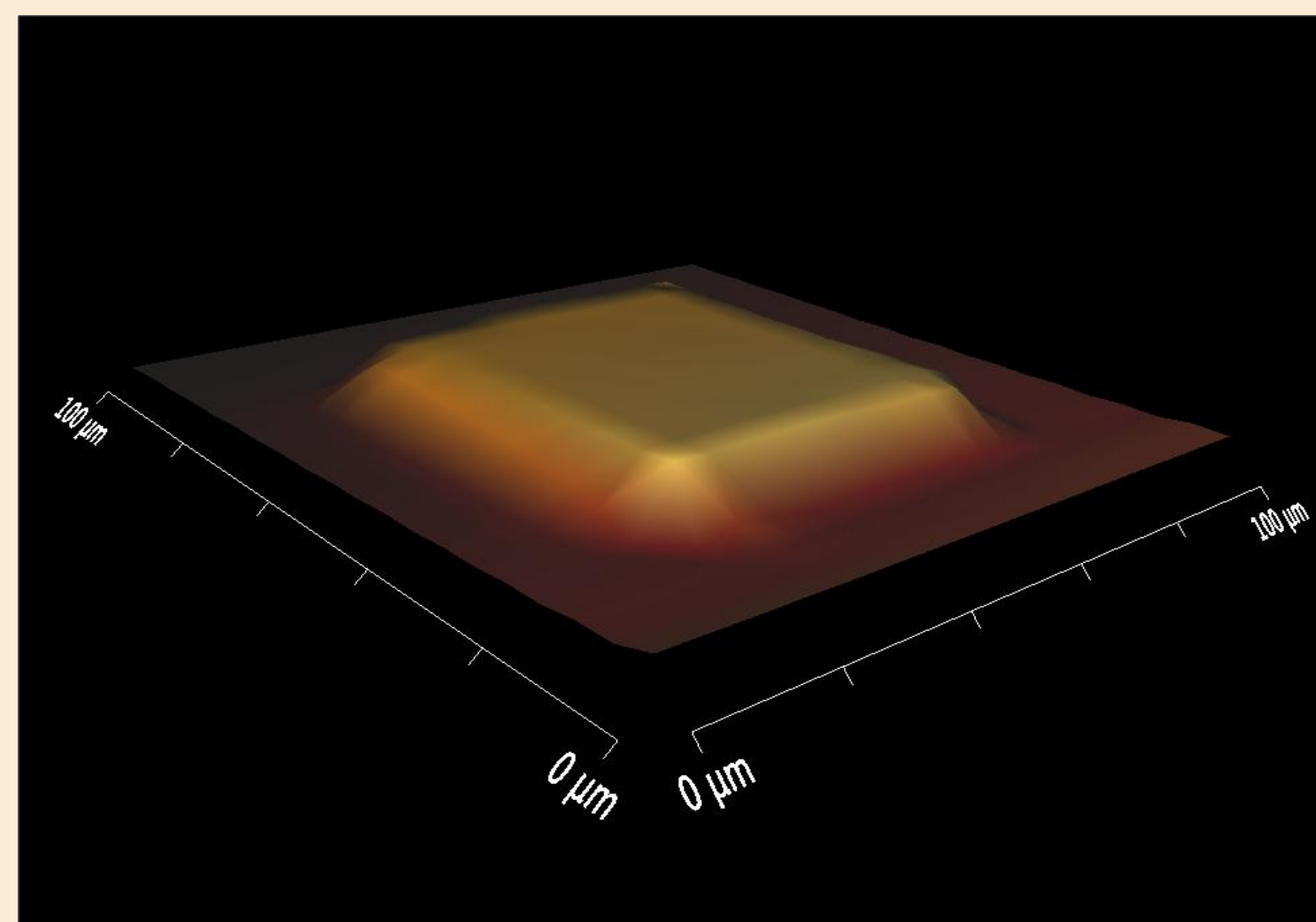


Fig. 4: 3D topology of developed sample

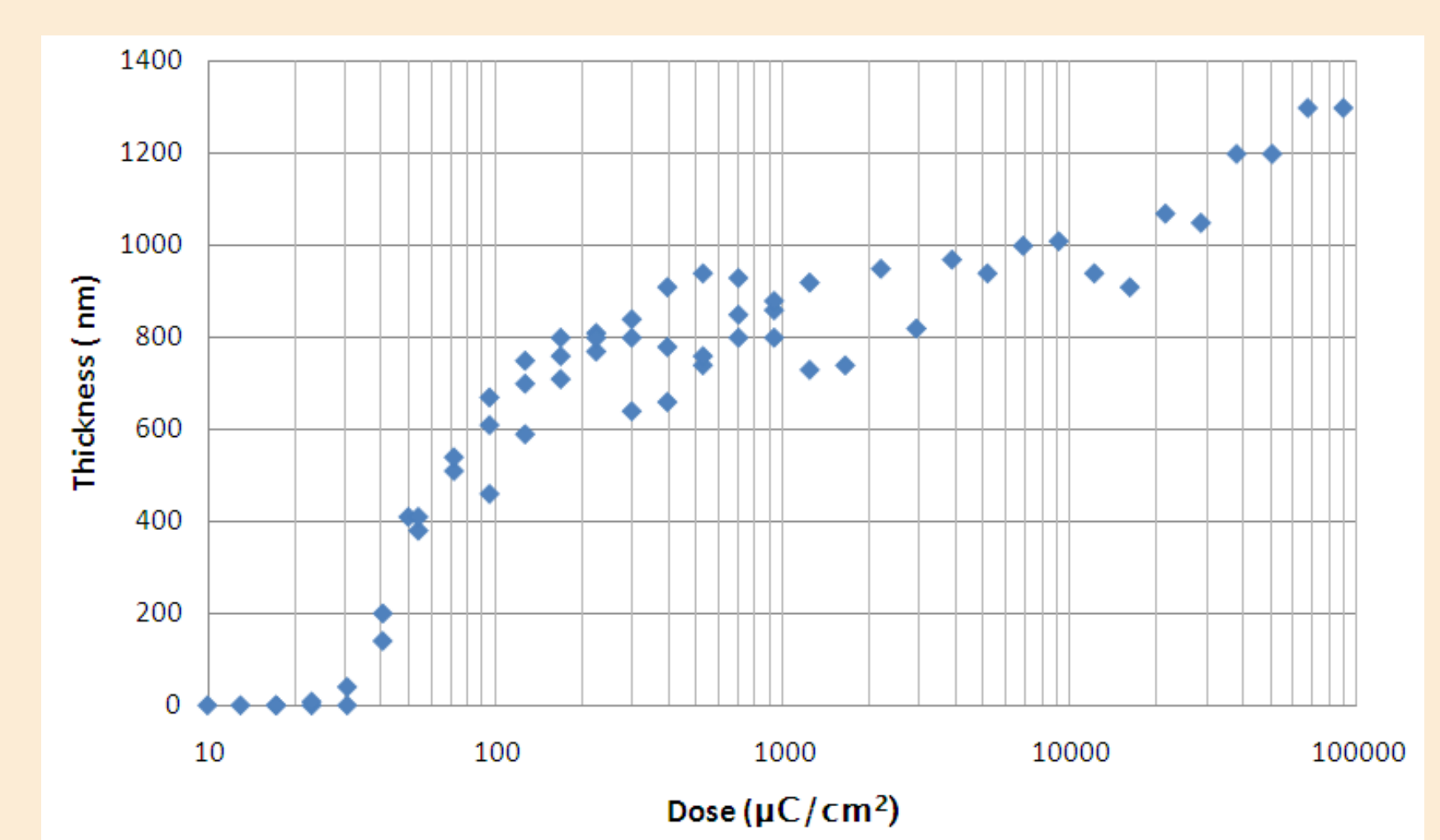


Fig. 5: Effect of dose on resulting film thickness

## Raman Spectroscopy

Large areas of approximately 1 x 1.3 mm were irradiated with electron doses of between 10 and 45,000  $\mu\text{C}/\text{cm}^2$ , at a beam energy of 30 keV and beam currents of between 21 and 760 nA. (The XL30 final aperture was opened to increase beam current allowing faster exposures of the extremely large areas required for Raman measurements. The unexposed material was not removed prior to spectroscopy. Raman spectra of specimens were obtained using a WiTec Alpha 300R (LOT Oriel, UK) operating a 0.3 W single frequency 785 nm diode laser (Toptica Photonics, Germany) and an Acton SP2300 triple grating monochromator/spectrograph (Princeton Instruments, USA) over the wavenumber range 200 – 3,000  $\text{cm}^{-1}$  at a mean resolution of 3  $\text{cm}^{-1}$ . Mean spectra were composed of 100 accumulations, acquiring individual spectra using an integration time of 0.2 s.

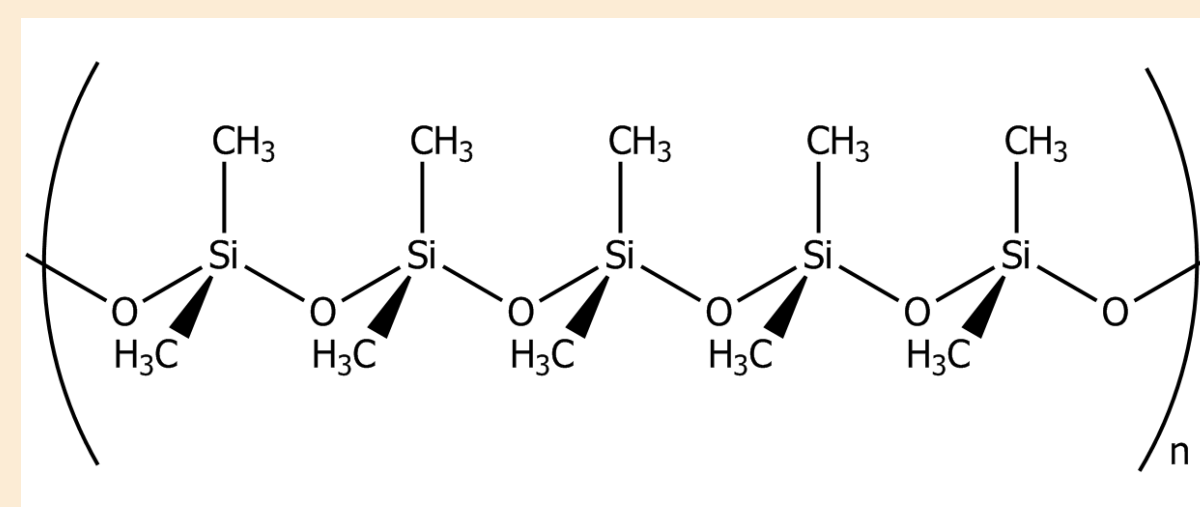


Fig. 6: Schematic of section of PDMS polymer chain

The chemical composition of PDMS is shown in Fig. 6. During irradiation, methyl groups are removed allowing the backbones of different polymer chains to become cross-linked. However, at large doses, the electrons also can cause chain scission and cause other chemical species to form. This is what is observed in Figs. 3 and 5 where we see liquid like PDMS below c.a. 150  $\mu\text{C}/\text{cm}^2$ , solidified PDMS between 150 and 3000  $\mu\text{C}/\text{cm}^2$  and swelling effects above 3000  $\mu\text{C}/\text{cm}^2$ . These bond formations and scissions corresponding to changes in phase may be perceptible in the Raman data. The results of the Raman analysis on samples with doses ranging from unexposed to 27571.7  $\mu\text{C}/\text{cm}^2$  is shown in Fig. 7. There are small peaks forming at higher doses in the highlighted areas in Fig. 7, and while they are weak, they are persistent, suggesting possible new bonds. This will form the basis of future analysis.

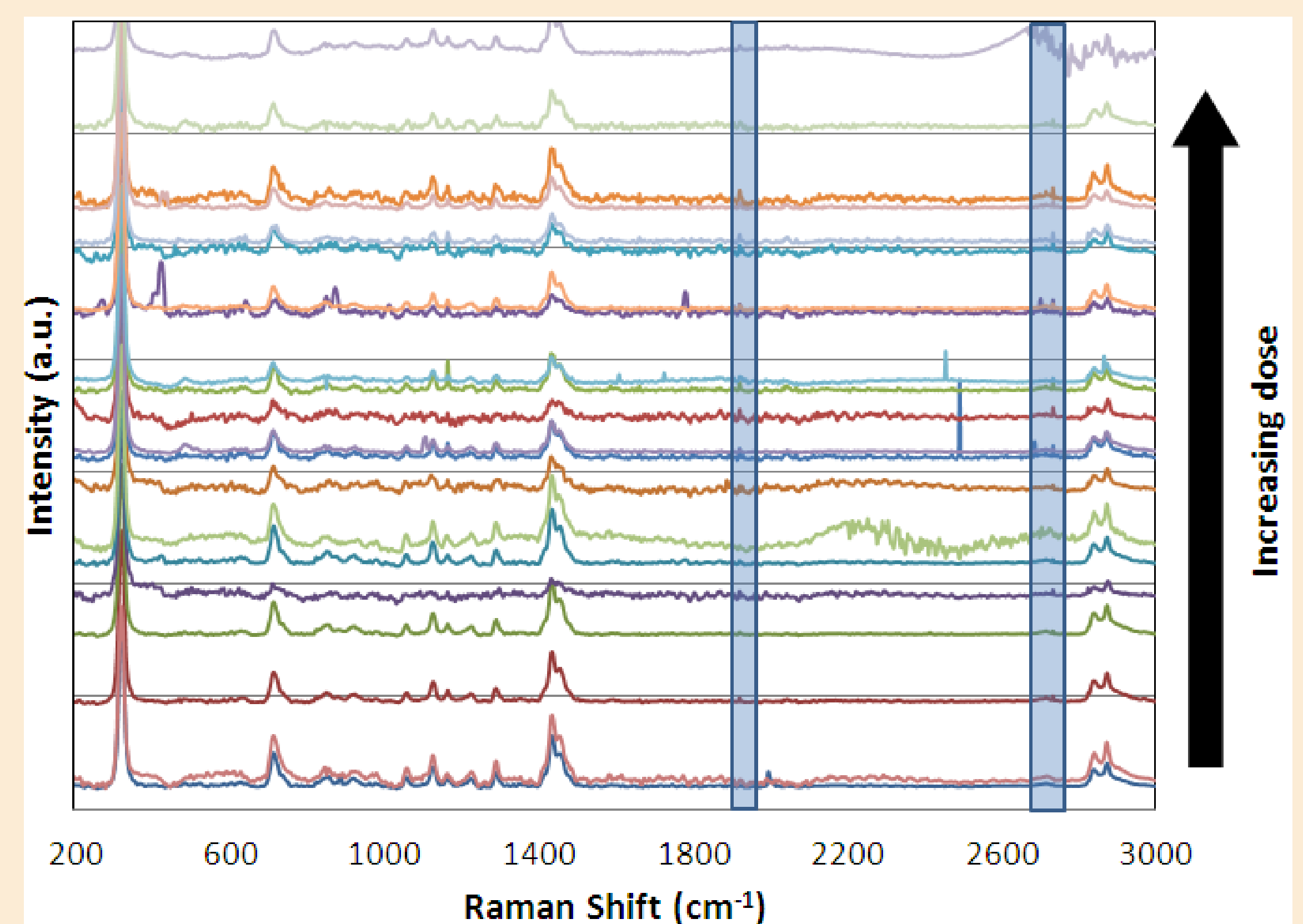


Fig. 7: Raman spectra – highlighted areas denote regions of interest

## Acknowledgements

Lithography was carried out in the Microfabrication Facility supported by Birmingham Science City: Creating and Characterising the Next Generation of Advanced Materials (West Midlands Centre for Advanced Materials Project 1). The Atomic Force Microscope and Confocal Raman Microscope used in this research were obtained, through Birmingham Science City: Innovative Uses for Advanced Materials in the Modern World (West Midlands Centre for Advanced Materials Project 2), with support from Advantage West Midlands (AWM) and part funded by the European Regional Development Fund (ERDF).

## References

- [1] A. Qaltieri, F. Pisanello, M. Grande, T. Stomeo, L. Martiradonna, G. Epifani, A. Fiore, A. Passaseo, M. De Vittorio, *Microelec. Eng.* 84 (2010) 1435-1438
- [2] E. Babich, J. Paraszczak, M. Hatzakis, J. Shaw, B.J. Grenon, *Microelec. Eng.* 3(1-4) (1985) 279-291
- [3] V. Constantoudis, E. Gogolides, A. Tserepi, D. Diakoumakos, E. S. Valamontes, *Microelec. Eng.* 61-62, (2002) 793-801
- [4] M. Morita, S., Imamura, A. Tanaka, T. Tamamura, *J. Electrochem. Soc.* (1984) 131(10) 2402-2406
- [5] T. Ito, M. Sakata, A. Endo, H. Jinbo, I. Ashida, *Jpn. J. Appl. Phys.* (1993) 32(12B-1) 6052-6058
- [6] A. A. S. Bhagat, P. Jothimuthu, I. Papautsky, *Lab Chip*, 7 (2007) 1192-1197
- [7] J. Bowen, D. Cheneler, D. Walliman, S.G. Arkless, Z. Zhang, M.C.L. Ward, M.J. Adams, *Meas. Sci. Technol.* 21 (2010) 115106